THE EFFECT OF BEAM-DRIVEN RETURN CURRENT INSTABILITY ON SOLAR HARD X-RAY BURSTS

D. Cromwell, P. McQuillan, and J. C. Brown

Departments of Astronomy and Natural Philosophy
University of Glasgow
Glasgow, G12 8QW, U.K.

ABSTRACT

The problem of electrostatic wave generation by a return current driven by a small area electron beam during solar hard X-ray bursts is discussed. The marginal stability method (cf. Duijveman et al. 1981) is used to solve numerically the electron and ion heating equations for a prescribed beam current evolution. When ion-acoustic waves are considered, we find that the method appears satisfactory and, following an initial phase of Coulomb resistivity in which T_e/T_i rises, predicts a rapid heating of substantial plasma volumes by anomalous ohmic dissipation. This hot plasma emits so much thermal bremsstrahlung that, contrary to previous expectations, the unstable beam-plasma system actually emits more hard X-rays than does the beam in the purely collisional thick target regime relevant to larger injection areas. Inclusion of ion-cyclotron waves results in ion-acoustic wave onset at lower T_e/T_i and a marginal stability treatment yields unphysical results. Specifically, negative resistivity occurs when the ion-acoustic instability is excited at an electron-to-ion temperature ratio of $T_e/T_i \lesssim 4{\cdot}5$, showing the marginal stability analysis of ion acoustic waves to be invalid in this regime. Discarding marginal stability and adopting a simple wave-energy equation, the time-dependent effect of ion-acoustic turbulence generated by the return current is investigated.

1 Introduction

It is commonly believed that electron beams, propagating downwards in the solar atmosphere, play a major role in the production, by collisional bremsstrahlung, of hard X-ray bursts during the impulsive phase of solar flares (see review by Brown and Smith 1980) and that they may also be

instrumental in flare atmospheric heating. In addition, it is recognised (e.g. Hoyng, Brown and van Beek 1976) that the large electron flux, demanded by the observed X-ray photon flux in such an interpretation, requires that a beam-neutralising return current be set up, such that:

$$\frac{n_b}{n_p} = \frac{v_d}{v_b} \qquad (1)$$

where $\frac{n_b}{n_p}$ is the ratio of beam density to ambient plasma density, v_b is the (sub-relativistic) beam velocity (a beam with single injection energy E_o, representing the mean energy of a real beam, is considered here) and v_d is the drift velocity of the ambient plasma electrons (which constitute the return current). If we consider, for simplicity, a model in which v_d increases during the impulsive phase, due to the rising beam flux $n_b v_b$, threshold velocities for the generation of various microinstabilities may be reached and so unstable wave growth may take place in the atmosphere. The resultant anomalous resistivity will affect hard X-ray production in two ways:

(a) The electric field required to drive the return current will increase and so reduce the lifetime of beam electrons. The nonthermal bremsstrahlung efficiency, which is already small, is therefore further reduced.

(b) Enhanced plasma heating will take place and thereby affect the observed thermal radiation signature.

The aim of this paper, then, is to describe preliminary results of calculations attempting to determine the effect of such return current instability on hard X-ray bursts during solar flares.

2 Marginal Stability Analysis

We consider a quasi-steady state consisting of a monoenergetic driving electron beam, with specified current density $j_b(t)$, current neutralising ($j_p = -j_b$) hot drifting electrons at temperature T_e, and hot stationary ions at temperature T_i. While recognising the possibility of beam-return current interaction, we concentrate here on the return current electron-background ion instability. The quasi-linear relaxation of the electron beam is considered elsewhere in these proceedings by McClements et al.

A typical large solar flare value is chosen for the peak total electron injection rate, $\mathcal{F}_o(s^{-1})$, but the beam area, A, is taken to be well below the upper limit set by hard X-ray images in order to ensure that unstable return current drift velocity thresholds are exceeded before this peak, viz.

$$\mathcal{F}_o = 10^{36} s^{-1}; \quad A = 10^{16} cm^2 \qquad (2)$$

(Brown and Melrose 1977, Hoyng, Knight and Spicer 1978). If we assume that this rate (2) is obtained after a linear increase over 10s, a typical time-scale for the impulsive phase, then our specified $j_b(t)$ is:

$$j_b(t) = 5.10^9 t \quad \text{statamp cm}^{-2} \qquad (3).$$

The electron beam is decelerated by the electric field that drives the return current and ignoring electron time-of-flight effects, it has a "stopping length", s (Brown and Hayward 1981) due to ohmic losses, given by

$$s = \frac{E_o}{e\eta j_b} \tag{4}$$

where E_o is the injected electron energy, here taken to be 100 keV and η is the resistivity of the plasma. Finally, we also assume a homogeneous and initially isothermal plasma with density $n_p = 10^{11}\text{cm}^{-3}$ and temperature $T_o = 5.10^6\,\text{K}$.

The heating equations for the plasma electrons and ions, neglecting collisional heating by the beam, and also convection, thermal conduction and radiation losses, are

$$\frac{3}{2} n_p \kappa \frac{dT_e}{dt} = \frac{3}{2} n_p \kappa \frac{(T_i - T_e)}{\tau} + \sum_i \chi_i \eta_i j_p^2 (t) \tag{5}$$

$$\frac{3}{2} n_p \kappa \frac{dT_i}{dt} = \frac{3}{2} n_p \kappa \frac{(T_e - T_i)}{\tau} + \sum_i (1 - \chi_i) \eta_i j_p^2 (t) \tag{6}$$

where κ is Boltzmann's constant, τ is the ion-electron energy exchange time, $\chi_i = \chi_i(T_e/T_i)$ and $(1 - \chi_i)$ are the fractions of the ohmic power dissipation $\eta_i j_p^2 (t)$ absorbed by the electrons and ions respectively as a result of collision process i, and η_i is the resistivity due to this process; e.g. in the case of classical Coulomb collisions, $\chi = 1$ and η is the usual Spitzer (1962) resistivity, proportional to $T_e^{-3/2}$.

With the onset of turbulence, anomalous resistivity sets in due to wave-particle collisions and so the ohmic heating term $\sum_i \eta_i j_p^2$ rises, leading to increased plasma heating. Note that this model, with a prescribed j(t), is fundamentally different from the Duijveman et al. (1981) problem where the electric field $\mathcal{E}(t)$ is specified. Specifically, their ohmic heating term, $\sum_i \frac{\mathcal{E}^2}{\eta_i}$, is reduced by any turbulent increase in η, a fact they appear to have overlooked. In other words, having a prescribed $\mathcal{E}$-field leads to reduced, rather than increased, plasma heating when anomalous resistivity sets in.

To solve equations (5) and (6) for $T_e(t)$, $T_i(t)$ and $\eta(t)$ we use the hypothesis of marginal stability (Manheimer and Boris 1977). States of marginal stability (i.e. states with zero growth-rate) in the present case can be represented by critical drift velocity (v_{crit}) curves in the $\left(\frac{v_d}{v_e}, \frac{T_e}{T_i}\right)$ plane, where $v_e = \left(\frac{\kappa T_e}{m_e}\right)^{1/2}$ is the electron thermal speed. We apply the marginal stability hypothesis by setting $v_d = v_{crit}$ at onset of turbulence, thereby constraining the system to evolve thereafter along the marginal stability curve. This gives us a relationship between T_e and T_i which, using the forms of χ for ion-cyclotron (IC) and ion-acoustic (IA) waves derived by

Duijveman et al. (1981), then allows us to solve numerically the heating equations (5) and (6).

We first consider the simplest case of an unmagnetised plasma, i.e. zero B-field. Figure 1 shows the evolution of the plasma in the $\left(\frac{v_d}{v_e}, \frac{T_e}{T_i}\right)$ plane. In the initial phase of classical resistivity, collisions cause an increase in T_e/T_i, from its initial value of 1.0, while the drift velocity rises, until the IA marginal stability curve is reached. The system then evolves along the curve. Figure 2 shows the variation of the normalised resistivity with time, ion-acoustic turbulence switching on after about 6s. Finally, the increases in T_e and T_i are seen in Figure 3. These profiles relate only to a plasma layer of thickness s_{min}, $\simeq 5.10^9$cm (emission measure $n^2 A s_{min} \simeq 5.10^{47} cm^{-3}$), the smallest depth of beam penetration into the atmosphere, because it is this region which is heated continuously during the simulation. The final temperatures obtained ($T_e \simeq 300\ T_o$, $T_i \simeq 35\ T_o$) will tend to be reduced by losses (neglected here) but we should note that wave generation will reduce thermal conductivity by the same factor as the electrical conductivity.

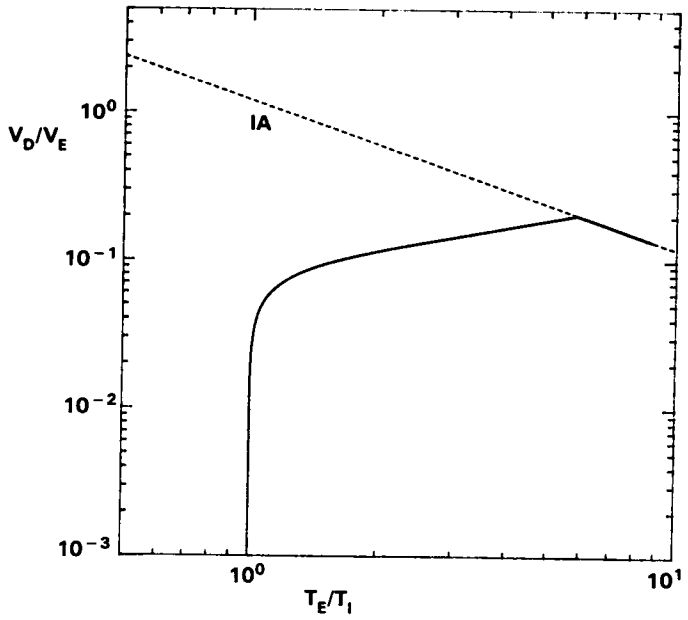

Figure 1. Evolution of the plasma in the $\left(\frac{v_d}{v_e} - \frac{T_e}{T_i}\right)$ plane, assuming marginal stability. IA denotes the ion-acoustic marginal stability curve.

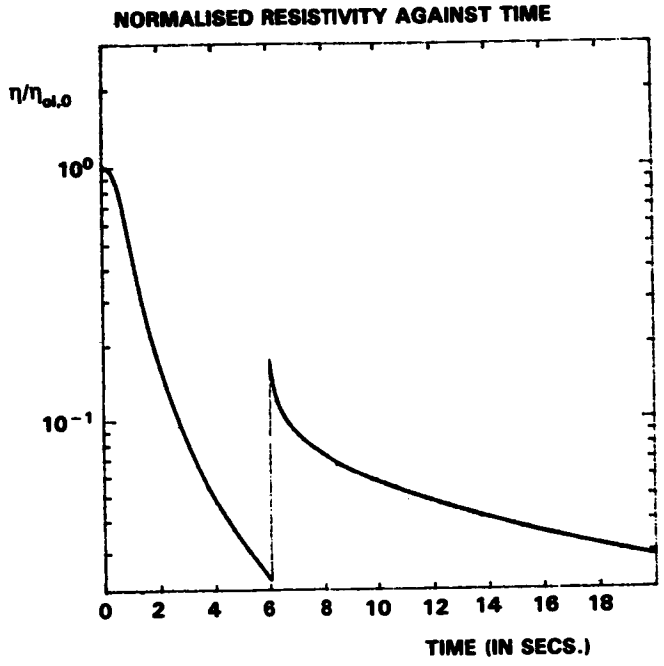

Figure 2. Variation of resistivity, normalised to the initial classical (i.e. Spitzer) resistivity. IA turbulence is generated at about 6s.

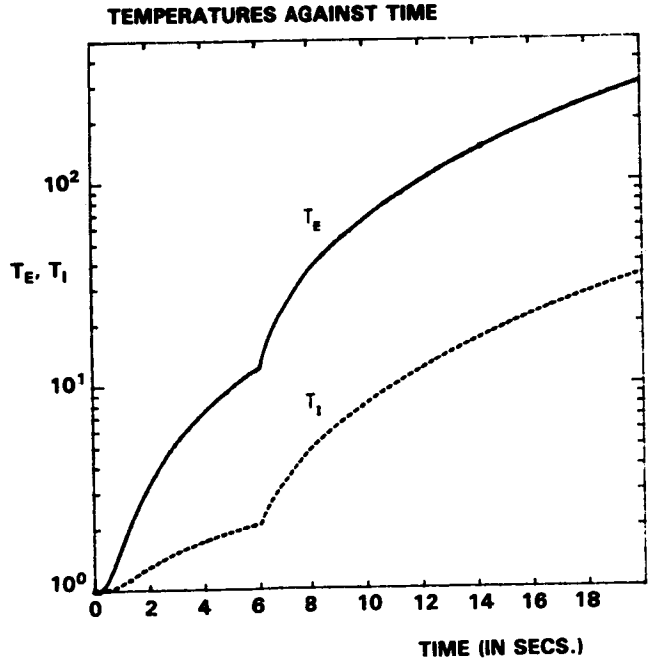

Figure 3. Rise in electron and ion temperatures, normalised to the initial temperature $T_o = 5.10^6 K$, showing the increases at onset of IA turbulence.

We now attempt to repeat the analysis for a magnetised plasma. For $T_e/T_i \lesssim 8$, the critical drift velocity for the generation of ion-cyclotron waves has the lowest threshold. These preferentially heat ions and so tend to reduce T_e/T_i. However they quickly saturate and do not contribute greatly to the total resistivity. The system then evolves away from the IC marginal stability curve, with T_e/T_i once again increasing due to the dominant effect of Coulomb collisions, until the IA marginal stability curve is reached. In this case, onset of IA turbulence occurs at lower T_e/T_i and we often find unphysical behaviour in the form of negative resistivity. Investigating further, by assuming a simple analytic form for the IA marginal stability curve and by using the form of $\chi_{IA} = \chi_{IA}(T_e/T_i)$ derived by Duijveman et al. (1981), we find that η is negative if $T_e/T_i \lesssim 4.5$. In other words, the application of marginal stability leads to negative values of anomalous resistivity, if the onset of ion-acoustic turbulence occurs at $T_e/T_i \lesssim 4.5$. We discuss this failure of marginal stability further in Section 5.

3 Wave Growth Analysis

In the previous discussion we did not incorporate any equations describing the growth of the ion-acoustic waves, which occurs on very short timescales in comparison to $v_d/\dot{v}_d$, the rise time of the return current. Here we adopt the following equation for the evolution of W, the wave energy,

$$\frac{dW}{dt} = \gamma W \tag{7}$$

where γ, the linear growth rate, is taken to be $10^{-2}\omega_{pi}$ (ω_{pi} is the ion plasma frequency). This growth rate corresponds to a drift velocity just in excess of the marginally stable drift velocity (Stringer 1964). Provided that $\frac{W}{n_p \kappa T_e} \ll 1$, (i.e. weak turbulence), we can relate the effective collision frequency, ν_{eff}, and the wave level using:

$$\nu_{eff} \simeq \omega_{pe} \frac{W}{n_p \kappa T_e} \tag{8}$$

(see, e.g. Hasegawa (1974)) where ω_{pe} is the electron plasma frequency. The effective (i.e. total, including classical) resistivity is then obtained using:

$$\eta_{eff} = \frac{4\pi \nu_{eff}}{\omega_{pe}^2} \tag{9}$$

(see, e.g. Papadopoulos 1977).

We can, therefore, solve equations (5) and (6) numerically in conjunction with equations (7), (8) and (9). The wave level grows from the thermal level, obtained by substituting the classical collision frequency in the left hand side of equation (8). There are several possible saturation mechanisms limit-

ing the growth of ion-acoustic waves (Hasegawa 1974) and the relevant process for solar flare conditions is by no means certain. Hasegawa gives three possible processes, the saturation level being lowest for the nonlinear two-wave interaction investigated by Tsytovich (1971). The effective collision frequency at saturation for this process is

$$\nu_{eff} \simeq 10^{-2}\ \omega_{pi}\ \frac{v_d}{c_s} \qquad (10)$$

where $c_s = \left(\frac{\kappa T_e}{m_i}\right)^{1/2}$ is the ion sound speed.

Our approach then, is to let classical heating proceed as v_d rises until the critical drift velocity for onset of ion-acoustic turbulence is reached. The wave energy then grows from the thermal level in the classical regime until saturation occurs. During the ion-acoustic heating phase, v_d/v_e decreases due to the rapid increase in T_e, until the system drops below the IA marginal stability curve (see Figure 4). The waves are then allowed to decay, with the same e-folding time ($1/\gamma$) as the wavegrowth, until the wave level has dropped to the thermal level, where, once again, classical heating only takes place.

Initial investigations show a rise in anomalous resistivity to $\sim 10^5$ times the initial classical value (see Figure 5), while T_e and T_i rise to $\sim 50\,T_o$ and $\sim 8\,T_o$ respectively (see Figure 6). These values are obtained in a very short time: the rise, saturation and decay of the IA waves takes place in $\sim 10^{-5}$ s. Again we note that the final temperature values are attained in the beam layer of thickness s_{min}, here found to be only $\simeq 3.5.10^3$ cm (emission measure $\simeq 3.5.10^{41}\text{cm}^{-3}$), because of the very high resistivity attained during IA turbulence. In our simulations, it is found that saturation occurs at $\frac{W}{\eta_p \kappa T_e} \simeq 10^{-3}$ thus satisfying the requirement for weak turbulence.

The above analysis has, of necessity, been a very simple approach to the problem. For example, a wave energy equation with a proper averaging over the wavenumber, k, of the wave spectrum W(k) would be more realistic. In addition, the controversial issue of the relevant saturation mechanism for solar flare parameters needs to be looked at in more detail.

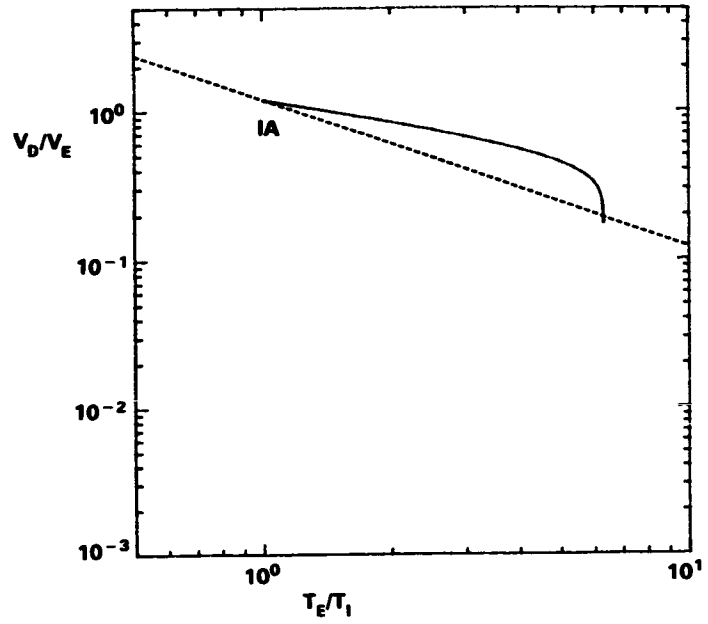

Figure 4. Evolution of the plasma in the $\left(\frac{v_d}{v_e} - \frac{T_e}{T_i}\right)$ plane using the wave growth analysis. The initial value of v_d is chosen such that the IA curve is reached after just a few numerical timesteps.

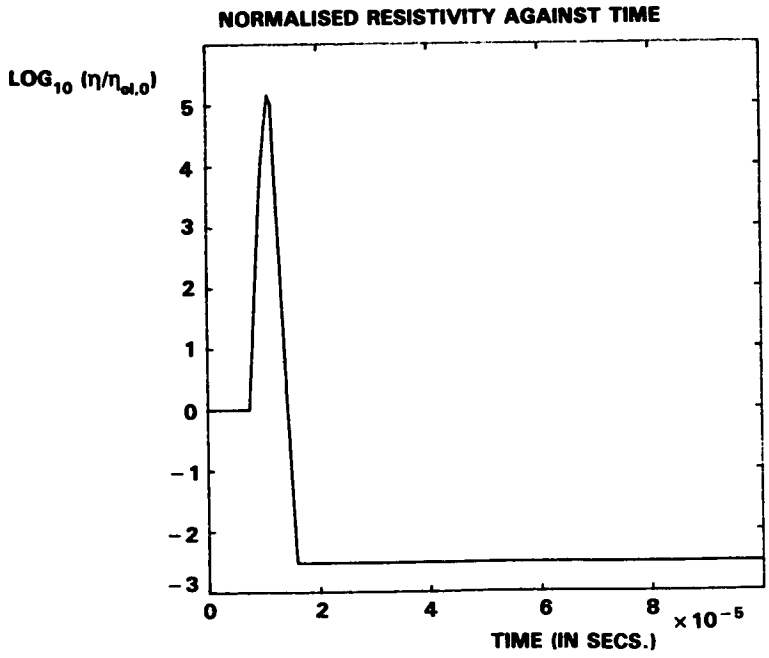

Figure 5. The variation of normalised resistivity with time, showing the growth, saturation and decay of IA resistivity in $\sim 10^{-5}$ s .

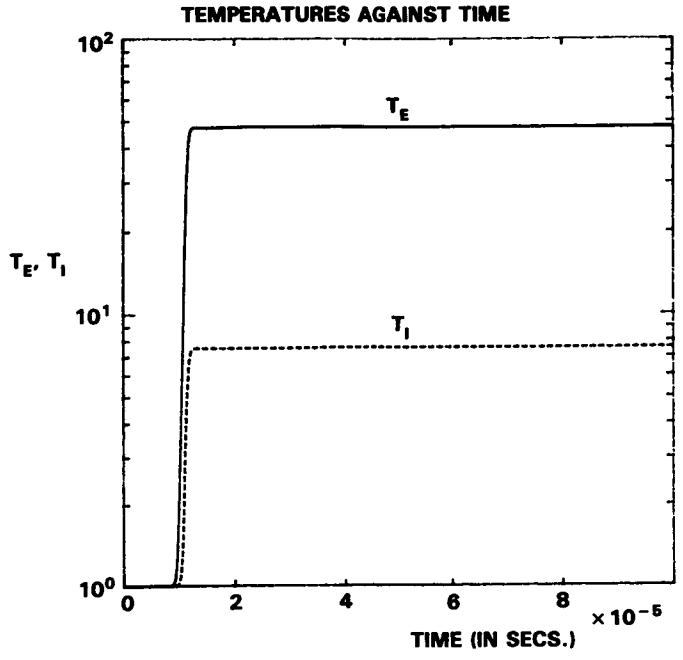

Figure 6. The electron and ion temperature profiles over the evolution time of 10^{-4} s.

4 The Effect of Return Current Instability on the Radiation Signature

In this section we briefly compare the thermal and non-thermal bremsstrahlung emitted at the instant when the beam has shrunk to its minimum length s_{min}. From equation (4) it can be seen that when η rises at onset of turbulence, the beam length is reduced by the same factor (over the short time-scale involved, the current density $j_b(t)$ is virtually constant). In other words, the electron beam lifetime is reduced and, correspondingly, the non-thermal bremsstrahlung. The enhanced ohmic dissipation of the return current, however, causes rapid local heating of the plasma and hence increases its thermal bremsstrahlung.

Below, we calculate the ratio of thermal to non-thermal radiation in the case of beam return current losses only, which as we will show, in some circumstances, dominate collisional losses from the beam when η is anomalous. For comparison, we also evaluate the ratio of the thermal bremsstrahlung in the anomalous case to the beam bremsstrahlung evaluated from the usual thick target formula which incorporates collisional losses only. The thermal emissivity from the volume $V = A.s_{min}$ is

$$\left(\frac{dJ}{d\varepsilon}\right)_T = Vn_p \int_{\varepsilon}^{\infty} v(E) \frac{dn}{dE} \frac{dQ}{d\varepsilon} (\varepsilon, E)\, dE \qquad (11)$$

where $\frac{dn}{dE}$, the number density of electrons per unit energy range, is given by

the Maxwellian distribution function and $\frac{dQ}{d\varepsilon}(\varepsilon, E)$ is the bremsstrahlung cross-section differential in photon energy. Here, as a simple first approximation, we assume Kramer's cross-section:

$$\frac{dQ}{d\varepsilon}(\varepsilon, E) = \frac{Q_o m_e c^2}{\varepsilon E} \tag{12}$$

where $Q_o = \frac{8}{3}\alpha r_e^2$ in the usual notation. The thick-target non-thermal emissivity (Brown 1971) is

$$\left(\frac{dJ}{d\varepsilon}\right)_{NT} = \int_{\varepsilon}^{\infty} \mathcal{J}(E)\nu(\varepsilon, E)\, dE \tag{13}$$

where $\mathcal{J}(E) = \mathcal{J}_o \delta(E - E_o)$ (s^{-1} per unit electron energy) is the electron flux and $\nu(\varepsilon, E)$ is the number of photons of energy ε emitted by an electron with initial energy E, given by:

$$\nu(\varepsilon, E) = n_p \int_{E_* = E}^{E_* = \varepsilon} \frac{dQ}{d\varepsilon}(\varepsilon, E_*) \frac{v(E_*)}{\left(\frac{dE_*}{dt}\right)} dE_* \tag{14}$$

In the case of beam losses due to ohmic dissipation of the return current only, the energy loss equation is

$$\frac{dE_*}{dt} = -e\mathcal{E}v(E_*) \tag{15}$$

where $\mathcal{E}$, the electric field, is given by

$$\mathcal{E} = e\eta \frac{\mathcal{J}_o}{A} \tag{16}.$$

The ratio of thermal to non-thermal emissivities (in the case of return current losses only) is then:

$$\frac{\left(\frac{dJ}{d\varepsilon}\right)_T}{\left(\frac{dJ}{d\varepsilon}\right)_{RC}} = \left(\frac{8}{\pi m_e \kappa T_e}\right)^{1/2} \frac{e^2 \eta n_p s_{min}}{\ell n\left(\frac{E_o}{\varepsilon}\right)} \exp\left(-\frac{\varepsilon}{\kappa T_e}\right) \tag{17}.$$

Equation (13) also applies to the case of beam Coulomb collisional losses only. The energy loss equation in this case is

$$\frac{dE_*}{dt} = -\frac{K n_p v(E_*)}{E_*} \tag{18}$$

where $K = 2\pi e^4 \Lambda$ in the usual notation. The ratio of thermal bremsstrahlung in the anomalous case to the non-thermal emissivity in the case of Coulomb collisional losses only is then:

$$\frac{\left(\frac{dJ}{d\varepsilon}\right)_T}{\left(\frac{dJ}{d\varepsilon}\right)_{CC}} = \left(\frac{8}{\pi m_e \kappa T_e}\right)^{1/2} \frac{n_p^2 \, VK}{\mathcal{F}_o (E_o - \varepsilon)} \qquad (19)$$

Applying equations (17) and (19) to the results of Section 2 (Marginal Stability) and Section 3 (Wave Growth Analysis) we find the following:

(a) Marginal stability analysis (Figures 1 - 3) gives, at ε = 20 keV:

$$\frac{\left(\frac{dJ}{d\varepsilon}\right)_T}{\left(\frac{dJ}{d\varepsilon}\right)_{RC}} \gtrsim 15 \; ; \quad \frac{\left(\frac{dJ}{d\varepsilon}\right)_T}{\left(\frac{dJ}{d\varepsilon}\right)_{CC}} \gtrsim 2.6 \qquad (20).$$

Here the thermal emissivity is over one order of magnitude greater than the non-thermal (return current) emissivity, and substantially exceeds that from a collisional thick target beam. Thus, when one considers a beam injection rate $\mathcal{F}_o$ and reduces the beam area, A, until the return current goes IA unstable, the beam length and bremsstrahlung are greatly reduced as usually assumed (e.g. Hoyng, Knight and Spicer 1978) but enhanced thermal bremsstrahlung from the rapidly heated plasma exceeds the thick target bremsstrahlung which is produced by the same beam over a large area A.

(b) Using the wave growth analysis (Figures 4 - 6), when unphysical behaviour is found in a marginal stability treatment, gives at ε = 20 keV:

$$\frac{\left(\frac{dJ}{d\varepsilon}\right)_T}{\left(\frac{dJ}{d\varepsilon}\right)_{RC}} \gtrsim 4 \; ; \quad \frac{\left(\frac{dJ}{d\varepsilon}\right)_T}{\left(\frac{dJ}{d\varepsilon}\right)_{CC}} \gtrsim 8.10^{-7} \qquad (21)$$

i.e. the thermal and return current non-thermal emissivities are comparable but the thermal emissivity is negligible in comparison with the collisional non-thermal emissivity. This is due to the small size of the emitting volume defined by s_{min}. In comparing these results with those of (a), we should note that the evolution time in each analysis is very different - 20s in the marginal stability case compared to 10^{-4} s in the wave growth case. However, we anticipate that over longer evolution times the wave growth analysis will result in a greater volume of material heated to $\sim 10^8$ K and a greater thermal emissivity (and emission measure).

5 The Failure of Marginal Stability

We return now to the problem of why the application of marginal stability leads in some cases to negative values of resistivity. There appears to be confusion in the literature as to whether or not there is a lower limit of T_e/T_i below which the ion-acoustic instability cannot be excited and therefore

below which the marginal stability curve used by us, by Duijveman et al. (1981) and by Holman (1985) for v_{crit} (IA) is irrelevant. For example, Kaplan, Pikel'ner and Tsytovich (1974) state quite explicitly (p.53) that "... it is necessary that $T_e \gtrsim 5T_i$" (for the growth of ion-acoustic waves). If this is correct, then it would be inappropriate to use our v_{crit} and χ - IA curves below $T_e/T_i \simeq 5$, and so it would not be surprising that unphysical results arise in this region. Similar statements are to be found in Melrose (1985) and in Stix (1962) (p.214) where a precise lower limit of $T_e/T_i \simeq 3.5$ is set. However all of these statements appear to be based on the assumption that $v_d << v_e$. In contrast, Fried and Gould (1961) and Kadomtsev (1965) state that the ion-acoustic instability can arise in an isothermal (i.e. $T_e/T_i \sim 1.0$) plasma if the drift velocity is high enough: $v_d \gtrsim v_e$.

By examining the roots of the linearised dispersion relation describing longitudinal plasma oscillations for drifting Maxwellians, we have ourselves confirmed the latter case: the so-called "ion-acoustic" mode will become unstable in an isothermal electron-ion plasma, described by drifting Maxwellians, if the relative drift velocity > $1.34v_e$. We hope to justify this in a subsequent paper. We are, of course, still left with the problem of explaining the failure of marginal stability for $T_e/T_i \lesssim 4.5$. It is possible that the form of the χ-function (Tange and Ichimaru, 1974) for ion-acoustic waves is the source of this difficulty and we intend to investigate this.

6 Discussions and Conclusions

We have presented a simple analysis of the problem of electrostatic wave generation by a beam-driven return current. The marginal stability approach fails below an electron-to-ion temperature ratio $T_e/T_i \simeq 4.5$. We believe that this is not due to any lower limit of T_e/T_i necessary for the generation of unstable ion-acoustic waves: the ion-acoustic instability will arise in an isothermal electron-ion plasma provided $v_d \gtrsim v_e$.

Both the marginal stability and wave growth analyses presented here allow us to calculate the uniform plasma heating only in the volume bounded by s_{min}, the minimum stopping length of the beam. A 2-D treatment of the combined spatial and temporal dependence is required to extend the problem to plasma heating outside this region. Future work should also incorporate a less idealised injected electron spectrum (e.g. power law). However, we believe that the essential result presented here of enhanced ohmic return current dissipation leading to rapid plasma heating to hard X-ray temperatures in milliseconds (i.e. typical spike burst durations) or less, will remain unaltered.

Acknowledgements

We would like to thank R. Bingham, E.W. Laing, A.L. MacKinnon and P.A. Sweet for helpful discussions relating to this paper. Two of us (D.C. and P.McQ.) gratefully acknowledge financial support from SERC.

References

Brown, J.C.: 1971, Solar Phys., 18, 489.
Brown, J.C. and Melrose, D.B.: 1977, Solar Phys., 52, 117.
Brown, J.C. and Smith, D.F.: 1980, Rep. Prog. Phys., 43, 125.
Brown, J.C. and Hayward, J.: 1981, Solar Phys., 73, 121.
Brown, J.C., Hayward, J. and Spicer, D.: 1981, Ap.J., 245, L91.
Duijveman, A., Hoyng, P. and Ionson, J.A.: 1981, Ap.J., 245, 721.
Fried, B.D. and Gould, R.W.: 1961, Phys. Fluids, 4, 139.
Hasegawa, A.: 1974, Rev. Geophys. Space Phys., 12, 273.
Holman, G.D.: 1985, Ap.J., 293, 584.
Hoyng, P., Brown, J.C. and van Beek, H.F.: 1976, Solar Phys., 48, 197.
Hoyng, P., Knight, J.W. and Spicer, D.S.: 1978, Solar Phys., 58, 139.
Kadomtsev, B.B.: 1965, "Plasma Turbulence", Academic Press (London).
Kaplan, S.A., Pikel'ner, S.B. and Tsytovich, V.N.: 1974, "Plasma Physics of the Solar Atmosphere", Physics Reports, Volume 15C, Number 1.
Manheimer, W. and Boris, J.P.: 1977, Comments Plasma Phys. Controlled Fusion, 3, 15.
Melrose, D.B.: 1985, in "Solar Radiophysics" (eds. D.J. McLean and N.R. Labrum), Cambridge University Press; Chapter 8.
Papadopoulos, K.: 1977, Rev. Geophys. Space Phys., 15, 113.
Spitzer, L.: 1962, "Physics of Fully Ionized Gases", Interscience (New York).
Stix, T.H.: 1962, "The Theory of Plasma Waves", McGraw-Hill (New York).
Stringer, T.E.: 1964, J. Nucl. Energy C6, 267.